Dephasing effects in molecular junction conduction: An analytical treatment

Zsolt Bihary and Mark A. Ratner
Department of Chemistry, Northwestern University, Evanston, Illinois 60208, USA
(Received 24 November 2004; revised manuscript received 2 August 2005; published 30 September 2005)

A Keldysh nonequilibrium Green's function approach is used in an analytic treatment of transport in oligomeric molecular wire junctions in the presence of dephasing effects. Both the dephasing and molecule-electrode interactions are treated using the self-energy formalism, and limiting analytic forms are obtained for the current as a function of dephasing strength, length, injection energy, molecular hopping integral, and temperature. Dephasing due to the interaction between electrons and thermal phonons is investigated in detail, and we relate the phenomenological dephasing parameter to the inner-sphere reorganization energy. In the single-site limit, we observe transitions in the spectral function from Lorentzian to semicircular as the dephasing strength increases, while for the extended chain we observe both tunneling and hopping behavior. In the limit of strong dephasing, the overall resistance can be expressed as the sum of the contact resistance and a chain-length-dependent hopping term.

DOI: 10.1103/PhysRevB.72.115439 PACS number(s): 73.63.Nm, 73.40.Cg, 73.23.Ad

I. INTRODUCTION

Current extensive activity in the general area of molecular electronics is focused on the behavior of molecular transport junctions, consisting of a few (ideally one) molecules assembled between metallic electrodes. For recent reviews, see Refs. 1–7. The conductance spectroscopy (current-voltage characteristics) of such structures has now been reported for a number of organic, organometallic, and oligomeric structures. Various limits of the transport have been observed, ranging from coherent tunneling transport in short-chain alkanes and few-ring structures[8–11] to the hopping limit in extended oligophenylenevinylenes.[12]

Theoretical analysis has largely been devoted to the coherent tunneling regime, where a series of electronic structure methods ranging from simple tight-binding models[13–17] to elaborate density functional techniques[18–23] have been used to characterize the transport. Extensive formal analysis has also been presented by several authors, analyzing the distance, temperature, and coupling dependences of the transport mechanism.[24–32] In particular, the transition from coherent to hopping transport has been demonstrated in several different ways. In the limit of strong vibronic coupling, the transport is expected to be of hopping type, and with sufficiently strong coupling and appropriate current densities, one can observe both a Franck-Condon set of vibrational levels[33] and actual bond fracture due to transporting electrons.[34–36] Most recently, inelastic tunneling spectroscopy (IETS) experiments have been completed, demonstrating vibronic coupling between vibrations of the extended molecule and electronic transport.[37–39] Theoretical analysis of such coupling has been presented, based both on simple perturbative analysis[40–43] and on a more complex self-consistent treatment of the vibronic and electrode couplings.[44,45]

Because tunneling spectroscopy measurements are inherently nonequilibrium (different chemical potentials of the two electrodes) and always occur in the presence of an external bath (the electrode energy levels themselves, as well as the vibrational levels of the molecular bridge and whatever environment may be present), full theoretical treatment of the transport must involve both a nonequilibrium method and a system-bath analysis. The preferred language for such a theoretical analysis is the Keldysh nonequilibrium Green's function method, which has been widely applied in the area.[2,7,20,21,46–49] In the current contribution, we utilize the Keldysh approach coupled with a very simple tight-binding model for transport through the molecular bridge itself. The aim is not a quantitative analysis of any given system, but rather a more general treatment of transport behavior and how limiting cases occur.

The Hamiltonian system itself is taken as the molecular bridge, treated in a Huckel model. Self-energies arise from the molecule-electrode couplings and from the vibronic coupling. We treat the latter as a thermal bath and investigate the consequences of electron-phonon coupling in a local energy representation. This permits a general expression for current in terms of coherent and incoherent contributions, which is expressed in terms of scattering superoperators. Various limiting cases can then be analyzed: in the single-site case, we find that the spectral function evolves from the Lorentzian form in the limit of weak dephasing to a semicircular structure for strong dephasing. With longer bridges and considering dephasing that is local both in space and in energy, we find a resistance structure that can be expressed in terms of the sum of the contact resistance term and the molecular contribution. The former is dependent on the contact couplings and proportional to the square root of the coupling strength, while the latter is proportional both to the coupling strength and to the length of the bridge and inversely proportional to a squared tunneling term.

The treatment is fully analytic and demonstrates both the utility of the Keldysh form in understanding the limits of molecular junction behavior and the mechanistic variations expected in simple oligomeric structures. The paper is organized as follows. In the next section we present a brief review of the Keldysh formalism and outline the model we used to represent the molecular junction. We derive the phenomenological dephasing self-energy term in Sec. III. General results are presented in Sec. IV, and we study the one-

site model in Sec. V. In Sec. VI we show how the present formulation leads to the noncoherent hopping behavior in the limit of strong dephasing, and in Sec. VII conclusions are given.

II. FORMALISM AND MODEL

We use the nonequilibrium Green function (NEGF) formalism. Although there are many excellent reviews available in the literature on this topic,[2,7,20,21,46–49] we briefly outline the methodology for the sake of clarity and to establish our notations. We are restricting ourselves to the study of stationary transport and work in the energy representation. We assume the existence of a well-defined self-energy. The aim is to solve the Dyson and Keldysh equations for the electronic Green functions:

$$G^r(E) = [E - H - \Sigma^r(E)]^{-1}, \tag{1}$$

$$G^a(E) = [E - H - \Sigma^a(E)]^{-1} = [G^r(E)]^+, \tag{2}$$

$$G^<(E) = G^r(E)\Sigma^<(E)G^a(E), \tag{3}$$

$$G^>(E) = G^r(E)\Sigma^>(E)G^a(E). \tag{4}$$

H is the Hamiltonian, $G^r(E)$, $G^a(E)$, $G^<(E)$, and $G^>(E)$ are the retarded, advanced, lesser, and greater Green functions, and $\Sigma^r(E)$, $\Sigma^a(E)$, $\Sigma^<(E)$, and $\Sigma^>(E)$ are the corresponding self-energies. We use the Huckel (tight-binding) model to describe the molecular system. The basis for electronic states is a set of spatially localized orbitals that may be considered atomic orbitals, or orbitals associated with different group of atoms, "sites" within the molecule.

The Hamiltonian in second quantized notation is

$$H = \sum_{i,j} t_{ij}\hat{a}_i^\dagger \hat{a}_j, \tag{5}$$

where $\hat{a}_i^\dagger(\hat{a}_i)$ describes the creation (annihilation) of an electron at site i in the molecule. In this paper we will investigate homogeneous, one-dimensional, single-band models defined by the Hamiltonian

$$H_{1D} = \varepsilon\sum_{i=1}^{n} \hat{a}_i^\dagger \hat{a}_i - t\sum_{i=1}^{n-1} (\hat{a}_i^\dagger \hat{a}_{i+1} + \hat{a}_{i+1}^\dagger \hat{a}_i). \tag{6}$$

Here, n is the number of sites, ε is the energy of the sites, and t is the hopping parameter. The conventional negative sign is used in the Hamiltonian to energetically favor long-wave-length molecular states. The Hamiltonian, the Green functions, and the self-energies can all be represented by matrices, using the atomic basis (this corresponds to real-space representation). The self-energies contain terms due to the leads (contacts) and also due to internal interactions, such as coupling to thermal phonons:

$$\Sigma^{r,a,<,>} = \Sigma_{lead}^{r,a,<,>} + \Sigma_{ph}^{r,a,<,>} = \Sigma_1^{r,a,<,>} + \Sigma_2^{r,a,<,>} + \Sigma_{ph}^{r,a,<,>}. \tag{7}$$

Σ_1 and Σ_2 refer to the two leads (source and drain). We take the contacts into account with self-energy terms in the wide-band limit:

$$\Sigma_{1(2)}^r = -\frac{i}{2}\Gamma_{1(2)}, \tag{8}$$

$$\Sigma_{1(2)}^a = +\frac{i}{2}\Gamma_{1(2)}, \tag{9}$$

$$\Sigma_{1(2)}^< = +i\Gamma_{1(2)}f_{1(2)}(E), \tag{10}$$

$$\Sigma_{1(2)}^> = -i\Gamma_{1(2)}[1 - f_{1(2)}(E)], \tag{11}$$

where $\Gamma_{1(2)}$ is the escape rate matrix and $f_{1(2)}(E)$ is the Fermi-Dirac distribution characterized by the chemical potential in the corresponding leads. For the specific models in this paper, we will assume the rate matrices couple only to the ends of the molecular chain:

$$[\Gamma_1]_{ij} = \Gamma_1\delta_{1i}\delta_{ij}, \tag{12}$$

$$[\Gamma_2]_{ij} = \Gamma_2\delta_{ni}\delta_{ij}; \tag{13}$$

now, $\Gamma_{1(2)}$ is simply the rate constant characterizing the coupling strength to the source (drain) contact.

We also want to take internal interactions into account, so we develop phenomenological self-energy terms due to high-temperature phonons in Sec. III. These internal self-energy terms in principle may depend on the Green functions, therefore Eqs. (1)–(4) need to be solved self-consistently. Once the Green functions have been obtained, together with the self-energies, they allow calculation of many important quantities. In particular, the spectral function is given as

$$A(E) = i[G^r(E) - G^a(E)] = i[G^>(E) - G^<(E)]. \tag{14}$$

The spectral function yields the density of states (DOS)

$$N(E) = \frac{1}{2\pi}\mathrm{Tr}[A(E)]. \tag{15}$$

The current transmitted through the junction is given as an integral of the flux of electrons at the source (or, equivalently, at the drain) over different energies:[49]

$$i(E) = \frac{e}{h}\mathrm{Tr}[\Sigma_1^<(E)G^>(E) - \Sigma_1^>(E)G^<(E)], \tag{16}$$

$$I = \int dE i(E). \tag{17}$$

Considering expressions (3) and (4) and breaking up the self-energies into their contact and phonon contributions, the Green functions can also be subdivided:

$$G^{<,>} = G^r\Sigma_{lead}^{<,>}G^a + G^r\Sigma_{ph}^{<,>}G^a. \tag{18}$$

The first term on the right-hand side (RHS) yields the elastic (coherent) part of the current, while the second gives rise to the noncoherent current when inserted into Eq. (16) Ref. 49:

$$i_{coh} = \frac{e}{h}\mathrm{Tr}[\Sigma_1^<G^r\Sigma_{lead}^>G^a - \Sigma_1^>G^r\Sigma_{lead}^<G^a], \tag{19}$$

$$i_{noncoh} = \frac{e}{h}\mathrm{Tr}[\Sigma_1^< G^r \Sigma_{ph}^> G^a - \Sigma_1^> G^r \Sigma_{ph}^< G^a]. \quad (20)$$

When internal interactions are neglected, the current is purely coherent and the formalism yields expressions that are consistent with the Landauer formula. Setting $\Sigma_{ph}^{<,>}=0$, using Eqs. (10) and (11), the electron flux can be written as

$$i = i_{coh} = \frac{e}{h}(f_1 - f_2)\mathrm{Tr}[\Gamma_1 G^r \Gamma_2 G^a] = \frac{e}{h}(f_1 - f_2)T, \quad (21)$$

where $T=\mathrm{Tr}[\Gamma_1 G^r \Gamma_2 G^a]$ is the transmission function.[13,17,49–55] When the leads are assumed to couple locally, at the ends of the molecular chain [such as defined by Eqs. (12) and (13)], the transmission function is related to the $1-n$ matrix element of G^r:

$$T = \Gamma_1 \Gamma_2 |[G^r]_{1n}|^2. \quad (22)$$

III. PHENOMENOLOGICAL MODEL FOR THE SELF-ENERGY DUE TO PHONONS IN THE HIGH-TEMPERATURE LIMIT

In this section we derive simple phenomenological forms for the self-energy terms induced by electron-phonon interactions. Most of the previous work in this respect has been devoted to the limit when the temperature is much lower than the phonon frequencies.[26] In this case, the transmitting electrons can only lose energy by phonon emission and the corresponding inelastic process yields resolved side peaks (phonon-peaks) in the transmission spectrum.[37,38,41,56] In this paper we are concerned with the opposite limit, when the temperature is larger than phonon frequencies and phonon absorption is as important as phonon emission. Our treatment is formally equivalent with that used for bulk materials,[57] but the final results of the section are developed for molecular systems.

We model the phonon bath as a collection of harmonic oscillators, with zeroth-order Hamiltonian ($\hbar=1$)

$$H_{ph} = \sum_k \omega_k \hat{b}_k^\dagger \hat{b}_k, \quad (23)$$

where $\hat{b}_k^\dagger(\hat{b}_k)$ are creation (annihilation) operators for independent phonons in the bath. The electron-phonon interaction is represented by the Hamiltonian of the Holstein model:

$$H_{el\text{-}ph} = \sum_{i,k} M_{ik} \hat{a}_i^\dagger \hat{a}_i \hat{B}_k, \quad (24)$$

where $\hat{B}_k=\hat{b}_k^\dagger+\hat{b}_k$. Polarization indices are incorporated in k. Within the self-consistent Born approximation, the self-energies then read[44,49,58–60]

$$[\Sigma_{ph}^r(E)]_{i,j} = i\sum_k M_{ik}M_{jk}\int \frac{d\omega}{2\pi}[D_k^<(\omega)G_{ij}^r(E-\omega) + D_k^r(\omega)G_{ij}^<(E-\omega) + D_k^r(\omega)G_{ij}^r(E-\omega)] + \delta_{ij}\sum_{k,i'} M_{ik}M_{i'k}n_{i'}^{el}D_k^r(\omega=0), \quad (25)$$

$$[\Sigma_{ph}^<(E)]_{i,j} = i\sum_k M_{ik}M_{jk}\int \frac{d\omega}{2\pi}D_k^<(\omega)G_{ij}^<(E-\omega), \quad (26)$$

$$[\Sigma_{ph}^>(E)]_{i,j} = i\sum_k M_{ik}M_{jk}\int \frac{d\omega}{2\pi}D_k^>(\omega)G_{ij}^>(E-\omega), \quad (27)$$

where $D_k^r(\omega)$, $D_k^<(\omega)$, and $D_k^>(\omega)$ are the retarded, lesser, and greater free-phonon Green functions, respectively, given as[61]

$$D_k^r(\omega) = \frac{1}{\omega-\omega_k+i\delta} - \frac{1}{\omega+\omega_k+i\delta}, \quad (28)$$

$$D_k^{\lessgtr}(\omega) = -2\pi i[(N_k+1)\delta(\omega\pm\omega_k) + N_k\delta(\omega\mp\omega_k)]. \quad (29)$$

Here, N_k is the occupation number for phonon mode k. In the proposed model we assume that the phonon spectrum and the phonon density of states are not changed due to the electron-phonon interaction and the phonon occupation numbers are calculated using the equilibrium distribution function at nonzero temperature. The Green functions (28) and (29) describe phonons with infinite lifetime, but this is not a crucial assumption; it only makes the algebra more transparent. The above expressions reveal that the lesser and greater functions are proportional to the occupation number, while the retarded function and the difference between the lesser and greater functions are not. In the limit of high occupation number (high-temperature limit compared to phonon frequencies) we assume the following inequalities: $D_k^r \ll D_k^< \approx D_k^>$. In this limit we can neglect terms in Eqs. (25)–(27) that involve $D_k^r(\omega)$ and we can substitute $D_k^>(\omega)$ with $D_k^<(\omega)$. We then obtain

$$[\Sigma_{ph}^{r,<,>}(E)]_{i,j} = i\sum_k M_{ik}M_{jk}\int \frac{d\omega}{2\pi}D_k^<(\omega)G_{ij}^{r,<,>}(E-\omega). \quad (30)$$

This result shows that in this limit each self-energy is related only to its corresponding Green function and through the same linear functional. This leads to conceptual and numerical simplification when Eqs. (1)–(4) are solved: The elements set of the four self-consistent matrix equations are decoupled. First we need to solve Eq. (1) for the retarded Green function, using the phenomenological formula (30), which relates the retarded self-energy only to the retarded Green function. The advanced function is simply given by the complex conjugate of the retarded function. Once the retarded and advanced Green functions have been determined, Eqs. (3) and (4) can be solved independently, using formula (30) again, this time for the lesser and greater self-energies. The general solution procedure therefore is broken up into first solving the Dyson equation, which governs the dynamics of the electron, and then solving the Keldysh kinetic equation. This simplification is similar to the case when internal interactions are totally neglected, but now both independent calculations need to be performed self-consistently. How high the temperature compared to phonon frequiencies needs to be in terms of reducing Eqs. (25)–(27)

to Eq. (30) is an interesting and important question that we cannot address here, but is worth further consideration.

To proceed, we make physically motivated assumptions about the way electrons are coupled to the phonon bath. Let us assume that each phonon mode is localized in the vicinity of a site, within a characteristic length ξ, but there is still a sufficient number of modes at each site to constitute a "local bath." The summation over the modes in Eq. (30) thus can be broken up into a summation over sites (k) and over modes at each site (ν). In a homogeneous model we may also assume that the local baths are the same at each site; i.e., the phonon Green function does not depend on k. We can now write Eq. (30) as

$$[\Sigma_{ph}^{r,<,>}(E)]_{i,j} = i\sum_k \sum_\nu M_{ik\nu}M_{jk\nu}\int \frac{d\omega}{2\pi} D_\nu^{<}(\omega)G_{ij}^{r,<,>}(E-\omega). \tag{31}$$

Only terms with simultaneous nonzero couplings $M_{ik\nu}$ and $M_{jk\nu}$ contribute to the sum, so the summation over k is effectively an overlap integral between sites i and j, which we assume drops to zero if the sites are farther apart than ξ. Following the usual procedure, we rewrite the summation over ν as an integral over phonon frequencies (assuming the coupling constants depend only on phonon frequency). We obtain

$$[\Sigma_{ph}^{r,<,>}(E)]_{i,j} = iR(|r_i - r_j|)\int d\omega_\nu M(\omega_\nu)^2 \times \rho(\omega_\nu)\int \frac{d\omega}{2\pi} D_\nu^{<}(\omega)G_{ij}^{r,<,>}(E-\omega), \tag{32}$$

where the distance-dependent function R drops to zero within the characteristic length ξ and $\rho(\omega_\nu)$ is the (local) density of phonon states. Substituting the expression for the high-temperature phonon Green function (using $N_k = k_BT/\hbar\omega_k$) we get

$$\begin{aligned}[\Sigma_{ph}^{r,<,>}(E)]_{i,j} &= k_BTR(|r_i - r_j|)\int_0^\infty d\omega_\nu M(\omega_\nu)^2 \\ &\times \rho(\omega_\nu)/\hbar\omega_\nu \int_{-\infty}^{\infty} d\omega\, \delta(\omega+\omega_\nu) + \delta(\omega \\ &- \omega_\nu)G_{ij}^{r,<,>}(E-\omega) \\ &= k_BTR(|r_i - r_j|)\int_{-\infty}^{\infty} d\omega M(\omega)^2\rho(\omega)G_{ij}^{r,<,>} \\ &(E-\omega)/\hbar\omega. \end{aligned} \tag{33}$$

We rewrite Eq. (33) for clarity as

$$[\Sigma_{ph}^{r,<,>}(E)]_{i,j} = DR(|r_i - r_j|)\int d\omega g(\omega)G_{ij}^{r,<,>}(E-\omega), \tag{34}$$

where

$$g(\omega) = \frac{M(\omega)^2\rho(\omega)/\hbar\omega}{\int d\omega M(\omega)^2\rho(\omega)/\hbar\omega},$$

$$D = k_BT\int d\omega M(\omega)^2\rho(\omega)/\hbar\omega. \tag{35}$$

Equation (34) is our phenomenological result for the phonon-induced self-energies in the high-temperature (high-phonon-occupation) limit. In Eq. (34),$R(|r_i-r_j|)$ is a (dimensionless, normalized) distance-dependent prefactor and $g(\omega)$ is the (normalized) spectral function for the electron-phonon coupling. In the present high-temperature limit, where phonon emission and phonon absorption are equally important, $g(\omega)$ is an even function and its range is restricted to the available phonon frequencies. The effective strength of the electron-phonon interaction is characterized by D, the dephasing strength. It is proportional to temperature and to the square of electron-phonon coupling (M). The magnitude of D can be estimated as

$$D \sim k_BT\frac{n\bar{M}^2}{\hbar\omega_D}, \tag{36}$$

where $\bar{M}$ is the typical value of the electron-phonon coupling in the system, n is the number of coupled phonons, and ω_D is the characteristic (Debye) frequency of the phonons. In the Marcus theory context, the fraction in Eq. (36) is related to the inner-sphere reorganization energy λ, as we will show: Consider first a single oscillator coupled to the electron. The force associated with the electron-phonon coupling energy [Eq. (24)] when an electron is added is $F=M/x_0$, where x_0 is the zero-point amplitude. The corresponding displacement is $\Delta x=F/f=M/(fx_0)$, where f is the force constant. Using the standard form for the reorganization energy in the case of a single coupled oscillator $\lambda=f/2(\Delta x)^2$,[62] we obtain $\lambda = M^2/(2fx_0^2)=M^2/(\hbar\omega)$. The fraction in Eq. (36) is a generalization for the multiphonon case. The dephasing parameter can thus also be written as $D\sim k_BT\lambda$, making it clear that D has units of energy squared. This important result allows us to estimate the value of D. Typical values for the reorganization energy in simple molecules are 0.1–0.6 eV,[63,64] while the thermal energy at room temperature is 0.025 eV, putting D in the 0.01-eV^2 regime.

The convolution over the phonon-frequencies in Eq. (34) reflects the possibility of energy exchange between the transmitted electron and the phonon bath. Let us investigate this mechanism in more detail with the help of Fig. 1(a). Electrons can transfer through the wire with different energies (the energy axis is shown vertical). Electrons both at higher and at lower energies (top and bottom lines) can scatter and contribute to the self-energy at the energy shown as the middle line. Assume that the Green function is a linearly changing (decreasing) function of the energy, as shown in Fig. 1(a). Because the self-energy contributions are proportional to the Green function, the contribution from the high-energy electron will in this case be smaller than that from the low-energy electron. However, as phonon emission and ab-

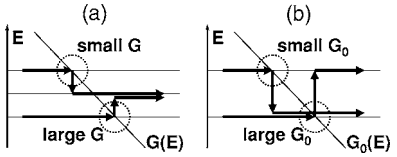

FIG. 1. Illustration of inelastic processes in the molecular wire. (a) The sum of self-energy contributions from phonon absorption and emission at a given energy is determined by the local value of the Green function. (b) More electrons scatter from large Green function (large DOS) energy channels to small DOS channels than vice versa. Electrons spectrally diffuse during transmission. See text for details.

sorption are equally important [$g(\omega)$ is symmetric] and we assumed a linear Green function, the sum of the contributions is simply determined by the value of the Green function at the average (middle) energy. In this case, Eq. (34) reduces to

$$[\Sigma_{ph}^{r,<,>}(E)]_{i,j} = DR(|r_i - r_j|)G_{ij}^{r,<,>}(E). \tag{37}$$

Far from the molecular resonances, the Green function is a smoothly varying function; therefore, Eq. (37) is a reasonable simplification. In regions where the Green function has substantial curvature, the approximation is questionable. The error can be estimated by Taylor expanding the Green functions (or, more conveniently, the spectral function) around E. At resonance with a Lorentzian peak with width parameter Γ, we get a relative error $(\omega_D/\Gamma)^2$. It shows that Eq. (37) is a reasonable approximation even in the case of resonance tunneling when the characteristic phonon frequency is much smaller than the escape rate associated with the resonance-peak.

Equation (37) is an important simplification: The relation between the Green functions and self-energies is now local in energy. The self-consistent Eqs. (1)–(4) can then be solved for each energy value independently; integration over the energy domain only occurs when calculating the terminal current. The form of Eq. (37) suggests that within this approximation, vertical transitions are disregarded; therefore, we refer to this phenomenology as the dephasing model. As our previous discussion shows, vertical transitions may still occur, but their effect is balanced in a sense that validates the energy local relation (37). On the other hand, even in this case, the internal interactions reshuffle electrons between different energies compared to the interaction-free situation. Figure 1(b) illustrates this point, showing the dephasing-free Green function in a small energy interval. Now consider a weak but nonzero interaction with the phonon bath. Electrons will scatter from the high-energy state to the low-energy state with a smaller rate than in the opposite direction, as the Green function in this example is smaller at higher energies. It is clear that the electron-phonon interaction rearranges, "spectrally diffuses" the transmitting electrons, from high-DOS regions to low-DOS regions. We shall see concrete examples for the consequences of this mechanism in later sections.

Considering the spatial dependence of the dephasing model, two opposite simple limits may be suggested: If the localization of phonons is strong, we may assume that overlap between them is restricted within each site—i.e., $R(|r_i - r_j|) = \delta_{ij}$. The self-energies are then diagonal matrices:

$$[\Sigma_{ph}^{r,<,>}(E)]_{i,j} = D\delta_{ij}G_{ij}^{r,<,>}(E). \tag{38}$$

On the other hand, if the correlation length of the phonons is greater than the entire chain, we may assume $R(|r_i - r_j|) = 1/n$ (n being the number of sites) and the self-energies now become

$$[\Sigma_{ph}^{r,<,>}(E)]_{i,j} = \frac{D}{n}G_{ij}^{r,<,>}(E). \tag{39}$$

We refer to this latter [Eq. (39)] phenomenology as the delocalized and to the former [Eq. (38)] as the local dephasing model. In the rest of the paper we will mainly focus our attention to the local dephasing model.

Finally, let us put our results in a more general context. The phenomenological self-energy formulas [Eqs. (34) and (37)–(39)] we obtained in this section were derived assuming an electron-phonon interaction as the main dephasing mechanism. However, Eq. (34) is also the most general phenomenological form for the self-energy under the reasonable simplifying assumptions that (a) the self-energy is a linear functional of the Green function, (b) each self-energy is related only to its corresponding Green function and through the same functional, and (c) the relation only depends on the distance between the sites. Equation (37) follows if we also assume that the relation is local in energy.

Due to its simplicity, the phenomenology discussed above can be used for other dephasing mechanisms. Indeed, self-energies with this functional form have been used to describe the effects of not only acoustic phonons, but also those of alloy fluctuations, interface roughness, and ionized dopants in layered semiconductor devices.[57] As a further example, one may consider a disordered chain, where the site energies are randomly detuned from their average value (e.g., as in a liquid or glassy environment). This (static) modulation corresponds to interactions with uncorrelated phonons in the limit of zero phonon frequencies; therefore, formula (38) should be a reasonable model in this case. For disordered chains, the dephasing parameter is temperature independent and is determined by the mean square of the detuning energy: $D \sim \langle \Delta\varepsilon^2 \rangle$.

IV. GENERAL RESULTS

As we saw in the previous section, it is reasonable to model the electronic self-energies due to a number of important dissipation mechanisms as a functional that relates the different self-energies only to their corresponding Green functions in a linear fashion:

$$\Sigma_{ph}^{r,<,>}(E) = \tilde{D}G^{r,<,>}(E). \tag{40}$$

The superoperator $\tilde{D}$ maps matrices to matrices and, in principle, may also involve energy convolution [see Eq. (34)]. Within the dephasing model, when vertical transitions are neglected (or their overall effect is balanced), $\tilde{D}$ is local in

energy [see Eq. (37)]. With the further assumption that the scattering centers are uncorrelated for different sites, the dephasing functional becomes local spatially as well as in energy; i.e., the self-energies become diagonal in the site representation [see Eq. (38)]. In this section we derive a number of general results starting from the formal relation (40).

A. Causality and charge conservation

Any phenomenological model for self-energies must obey the principle of causality, which means that in the time domain, the retarded (advanced) self-energy must be zero at negative (positive) times. The relation in Eq. (34) is a convolution in the frequency domain. Fourier transformation converts the relation into a simple product in the time domain: $[\Sigma^r_{ph}(\tau)]_{i,j}=DR(|r_i-r_j|)g(\tau)G^r_{ij}(\tau)$. Because $G^r_{ij}(\tau)$ does vanish at negative times, so does $\Sigma^r_{ph}(\tau)$, thus proving causality for the self-energy. A similar analysis shows that the relation $\Sigma^r_{ph}-\Sigma^a_{ph}=\Sigma^>_{ph}-\Sigma^<_{ph}$ holds.

As realized by Buttiker,[55] interactions can be viewed as processes involving the exchange of electrons with a conceptual reservoir. Next we demonstrate that our model, as it should, yields zero current associated with such processes. The flux of particles into the conceptual reservoir is[49]

$$i_{ph}(E)=\frac{e}{h}\mathrm{Tr}[G^>(E)\Sigma^<_{ph}(E)-G^<(E)\Sigma^>_{ph}(E)]$$
$$=\frac{e}{h}\mathrm{Tr}[G^>(E)\tilde{D}G^<(E)-G^<(E)\tilde{D}G^>(E)], \quad (41)$$

while the current to the reservoir is $\int i_{ph}(E)dE$. It vanishes due to the Hermitian property of $\tilde{D}$ in the sense that for any energy-dependent (matrix) functions $X(E)$ and $Y(E)$,

$$\int \mathrm{Tr}[X(E)\tilde{D}Y(E)]dE=\int \mathrm{Tr}[Y(E)\tilde{D}X(E)]dE. \quad (42)$$

$\tilde{D}$ possesses this property for all the specific models described in the previous section, and we may postulate it in the general case. Within the local dephasing model, it is easy to show that the electron flux to the reservoir is zero *at each energy and at each site*:

$$[G^>\tilde{D}G^<-G^<\tilde{D}G^>]_{ii}=[G^>]_{ii}D[G^<]_{ii}-[G^<]_{ii}D[G^>]_{ii}=0. \quad (43)$$

This conclusion again shows the underlying assumption in the dephasing model that the overall vertical flow of electrons is zero.

B. Terminal current, electron flux, and transmission function

Now we proceed to obtain the formal solution for the terminal current in the presence of internal processes. We will restrict the discussion to the dephasing model; i.e., the superoperator $\tilde{D}$ is assumed local in energy. As described in the previous section, first we need to solve the self-consistent matrix equation for the retarded Green function. Substituting expression (40) for $\Sigma^r_{ph}(E)$ into the Dyson equation (1) we obtain

$$G^r_D(E)=[E-H_{el}-\Sigma^r_{lead}-\tilde{D}G^r_D(E)]^{-1}. \quad (44)$$

The subscript D in the Green function reminds us of the presence of the dephasing processes. This nonlinear matrix equation has to be solved self-consistently. Within the dephasing model, $\tilde{D}$ does not mix Green functions at different energies, so equations for $G^r_D(E)$ at different values of E can be solved independently. The advanced Green function $G^a_D(E)$ is simply obtained as the Hermitian conjugate of $G^r_D(E)$. Next, we solve for the lesser and greater Green functions using Eqs. (3) and (4) and for the flux of electrons given by Eq. (16). Within the dephasing model, every quantity is local in energy; therefore, the terminal current is still given as the energy integral of the flux [see Eq. (17)], and the transmission function can still be defined as before. The coherent part of the flux is given in Eq. (19). Using Eqs. (10) and (11) we derive

$$i_{coh}=\frac{e}{h}(f_1-f_2)\mathrm{Tr}[\Gamma_1G^r_D\Gamma_2G^a_D]. \quad (45)$$

We define the coherent transmission as in Eq. (21), and from Eq. (45) we conclude

$$T_{coh}=\mathrm{Tr}[\Gamma_1G^r_D\Gamma_2G^a_D]. \quad (46)$$

The coherent transmission has exactly the same form as without dephasing [see Eq. (21)]; the effect of the dephasing processes enters only in the form for the retarded (and advanced) Green functions. For further development, let us define the propagator $\tilde{U}_D$, as a superoperator that acts on any matrix X as $\tilde{U}_DX=G^r_DXG^a_D$. Also, let us identify the trace of the matrix product, $\mathrm{Tr}[XY]$, as the scalar product of the two matrices: $\langle XY\rangle$. Now we can write the coherent transmission as

$$T_{coh}=\langle\Gamma_1\tilde{U}_D\Gamma_2\rangle. \quad (47)$$

The physical meaning of the above expression is clear: The coherent contribution to electron transmission is determined by the correlation between the contact operators Γ_1,Γ_2 through the propagator $\tilde{U}_D$.

In order to obtain the noncoherent flux (and transmission), we have to express the self-energies due to phonons. Using our phenomenological model, we can write

$$\Sigma^<_{ph}=\tilde{D}G^<$$
$$=\tilde{D}(G^r_D\Sigma^<G^a_D)$$
$$=\tilde{D}(G^r_D(\Sigma^<_{lead}+\Sigma^<_{ph})G^a_D)$$
$$=\tilde{D}\tilde{U}_D(\Sigma^<_{lead}+\Sigma^<_{ph}), \quad (48)$$

whose formal solution is

$$\Sigma_{ph}^{<} = \tilde{D}\tilde{U}_D(1-\tilde{D}\tilde{U}_D)^{-1}\Sigma_{lead}^{<}. \quad (49)$$

$\Sigma_{ph}^{>}$ is given by a similar expression. Using the definition [Eq. (20)] and the contact limits of Eqs. (10) and (11) and substituting Eq. (49), we arrive at the result

$$i_{noncoh} = \frac{e}{h}(f_1 - f_2)\langle \Gamma_1 \tilde{U}_D \tilde{D} \tilde{U}_D (1-\tilde{D}\tilde{U}_D)^{-1}\Gamma_2\rangle, \quad (50)$$

from which the noncoherent transmission can be defined as

$$T_{noncoh} = \langle \Gamma_1 \tilde{U}_D \tilde{D} \tilde{U}_D (1-\tilde{D}\tilde{U}_D)^{-1}\Gamma_2\rangle. \quad (51)$$

combining Eqs. (47) and (51) yields the total electron transmission:

$$T = T_{coh} + T_{noncoh} = \langle \Gamma_1 \tilde{U}_D (1-\tilde{D}\tilde{U}_D)^{-1}\Gamma_2\rangle. \quad (52)$$

We can see now that the total transmission is in a form that is very similar to the standard expression (47) obtained for the coherent part. The only difference is that now the superoperator describing the electron propagation (transmission) between the contacts is renormalized:

$$T = \langle \Gamma_1 \tilde{U}_D^{ren} \Gamma_2\rangle, \quad (53)$$

where

$$\tilde{U}^{ren} = \tilde{U}_D(1-\tilde{D}\tilde{U}_D)^{-1} = (1-\tilde{U}_D\tilde{D})^{-1}\tilde{U}_D. \quad (54)$$

To gain additional insight, let us expand the formal expression (52):

$$T = \langle \Gamma_1 (\tilde{U}_D + \tilde{U}_D\tilde{D}\tilde{U}_D + \tilde{U}_D\tilde{D}\tilde{U}_D\tilde{D}\tilde{U}_D + \cdots)\Gamma_2\rangle. \quad (55)$$

The physical meaning of this expansion is clear: The total transmission is determined by a sum of terms representing a growing number of scattering processes. The first term describes the propagation of the electron injected with Γ_1, correlating with the Γ_2 emitter. This gives the coherent part of the transmission. All the other terms contribute to the noncoherent part, describing a growing number of consecutive dephasing (scattering) events, connected with electron propagations. The subscript in $\tilde{U}_D$ is a reminder that the propagator is also affected by dephasing—the transmission is not simply an expansion in powers of $\tilde{D}$ as it may look at first glance. Our result is a slight generalization of the expansion obtained in Ref. 57 for semiconductor devices.

C. Transmission function with local dephasing and local couplings to the leads

We now derive general formulas for the coherent and total transmission functions assuming the local dephasing model [Eq. (38)] and local contacts [Eqs. (12) and (13)]. Within this model, the coherent transmission is given as usual by the simple formula

$$T_{coh} = \langle \Gamma_1 \tilde{U} \Gamma_2\rangle = \Gamma_1\Gamma_2 |[G^r]_{1n}|^2. \quad (56)$$

We now calculate the total transmission. The second term in Eq. (55) can be written as

$$\langle \Gamma_1 \tilde{U}\tilde{D}\tilde{U}\tilde{D}\tilde{U}\Gamma_2\rangle = \Gamma_1\Gamma_2 D \sum_k |[G^r]_{1k}|^2 |[G^r]_{kn}|^2. \quad (57)$$

Let us define the $n\times n$ matrix Q as

$$[Q]_{ij} = |[G^r]_{ij}|^2. \quad (58)$$

We can now rewrite Eqs. (56) and (57) as

$$\langle \Gamma_1 \tilde{U} \Gamma_2\rangle = \Gamma_1\Gamma_2 [Q]_{1n}, \quad (59)$$

$$\langle \Gamma_1 \tilde{U}\tilde{D}\tilde{U}\Gamma_2\rangle = \Gamma_1\Gamma_2 D [Q^2]_{1n}, \quad (60)$$

where $[Q^2]_{1n}$ is the $1-n$ element of the matrix $Q^2 = QQ$. It is not hard to prove the generalization of these formulas:

$$\langle \Gamma_1 (\tilde{U}\tilde{D})^k \tilde{U}\Gamma_2\rangle = \Gamma_1\Gamma_2 D^k [Q^{k+1}]_{1n}, \quad (61)$$

from which it follows that the total transmission can be written as

$$\begin{aligned} T &= \langle \Gamma_1 \tilde{U}(1-\tilde{D}\tilde{U})^{-1}\Gamma_2\rangle \\ &= \sum_{k=0}^{\infty} \Gamma_1\Gamma_2 [Q(DQ)^k]_{1n} \\ &= \Gamma_1\Gamma_2 [Q(1-DQ)^{-1}]_{1n}. \end{aligned} \quad (62)$$

When both the contacts and dephasing mechanism are local, the formal results obtained in the previous subsection are greatly simplified. The general formulas, involving superoperators, reduce to the $1-n$ element of an ordinary matrix. This result is the generalization of the well-known formula, Eq. (22) (which in the present context can be written as $T = \Gamma_1\Gamma_2[Q]_{1n}$), and is essentially equivalent to formulas obtained for semiconductor devices.[57]

V. ONE-SITE MODEL

The simplest model involves a single site with one electronic level between the contacts. All the operators and superoperators can be represented in this case by 1×1 matrices—i.e., by complex numbers. Choosing the energy reference at the energy of the single atomic orbital ($\varepsilon = 0$), the Hamiltonian is zero. The self-consistent equation for the retarded Green function becomes

$$G^r = (E + i\Gamma/2 - DG^r)^{-1}, \quad (63)$$

where $\Gamma = (\Gamma_1 + \Gamma_2)$, the sum of the rate constants. In the one-site model both terminals couple to the same site. Expression (63) can be solved explicitly. The root with the smaller magnitude is the physically relevant solution, as it corresponds to a stable fixed point of the self-consistent map (63). For further development, we write the solution in two equivalent, alternative forms

$$\begin{aligned} G^r &= \frac{E + i\Gamma/2 - \sqrt{(E+i\Gamma/2)^2 - 4D}}{2D} \\ &= \frac{2}{E + i\Gamma/2 + \sqrt{(E+i\Gamma/2)^2 - 4D}}. \end{aligned} \quad (64)$$

We can now compute the spectral function $A = i(G^r - G^a)$

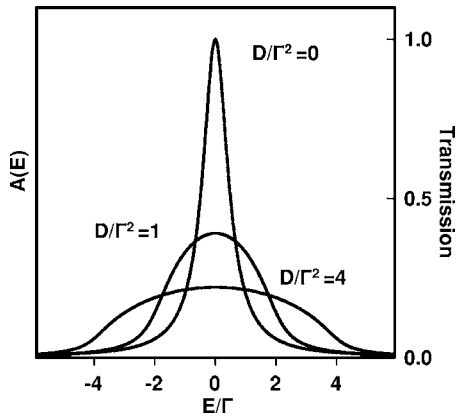

FIG. 2. Spectral function for the one-site model at different values of the (reduced) dephasing parameter D/Γ^2. The spectral function evolves from a Lorentzian to a semicircular form as D/Γ^2 is increased. For the one-site model, the transmission function is simply proportional to the spectral function; therefore, the curves also show the latter (for scale, see the vertical axis on the right).

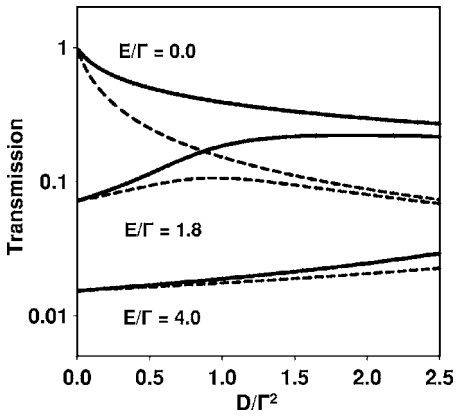

FIG. 3. Transmission functions versus (reduced) dephasing parameter for the one-site model at different (reduced) energies. Solid lines show total transmission; dashed lines show the coherent part of the transmission functions. The transmission axis is logarithmic.

$=-2\,\mathrm{Im}[G^r]$. In one dimension, the DOS is simply proportional to the spectral function $N(E)=A/2\pi$. Using the second line in Eq. (64), it is easy to consider the limit when dephasing effects may be neglected ($D\to 0$). The Green function then simplifies to $G^r=1/(E+i\Gamma/2)$, and we recover the well-known Lorentzian form for the spectral function:

$$A=\frac{\Gamma}{E^2+(\Gamma/2)^2}. \tag{65}$$

In the opposite limit, when dephasing effects are strong compared to the coupling to the leads ($\Gamma\to 0$), the spectral function takes a semicircular form

$$A=\frac{\sqrt{4D-E^2}}{D} \tag{66}$$

for values of E where the above expression is real (i.e., for $|E|<2\sqrt{D}$) and zero otherwise. The width of the "peak" is now determined by the dephasing parameter. This semicircular form is reminiscent of the spectral function obtained with random matrix techniques for homogeneous chains with diagonal random disorder.[65–67] As we discussed in Sec. III, the present dephasing model is indeed applicable to such randomly disordered chains. The only energy scale for the one-site model is set by Γ, and the relative significance of dephasing is characterized by the dimensionless fraction D/Γ^2. We plot the spectral function for various values of D/Γ^2 in Fig. 2. We can see that the peak value of the distribution decreases while its width grows with growing D and its shape changes from the Lorentzian to the semicircular form. While the molecule-electrode coupling depends very strongly on the geometry and chemical composition of the junction, $\Gamma=0.1$ eV can be considered a reasonable value. In the previous section we estimated D in the 0.01-eV^2 regime for a simple molecule at room temperatures. These values yield $D/\Gamma^2=1$, showing the physical relevance of our discussion in realistic experimental systems.

The Q matrix defined in Eq. (58) is now simply the real number $Q=|G^r|^2$. The general relationship $A=iG^r(\Sigma^r-\Sigma^a)G^a$ translates in our case to the equation $A=|G^r|^2(\Gamma+DA)$. It allows us to express the coherent and noncoherent transmission functions with the spectral function:

$$T_{coh}=\frac{\Gamma_1\Gamma_2 A}{\Gamma+DA}, \tag{67}$$

$$T_{noncoh}=\frac{\Gamma_1\Gamma_2 DA^2}{\Gamma(\Gamma+DA)}. \tag{68}$$

Their relative ratio is

$$\frac{T_{noncoh}}{T_{coh}}=\frac{DA}{\Gamma}. \tag{69}$$

This result is very intuitive: the noncoherent contribution becomes comparable to the coherent one when the dephasing rate in the sample, given by the product of the dephasing constant and the spectral function, becomes appreciable compared to the escape rates to the leads. The total transmission function $T=T_{coh}+T_{noncoh}$ can be written in a particularly simple form

$$T=\frac{\Gamma_1\Gamma_2}{\Gamma}A, \tag{70}$$

in accordance with the general result for systems with proportionate couplings. Because of this proportionality, the plots in Fig. 2 can be viewed also as transmission functions at different dephasing strengths (see the scale on the right vertical axis). On these plots, we assumed the junction is symmetric: $\Gamma_1=\Gamma_2=\Gamma/2$.

Figure 3 shows the total transmission (solid lines) and their coherent parts (dotted lines) as functions of the (dimensionless) dephasing parameter D/Γ^2 at different (dimensionless) energies. The rate constants were again assumed equal. The transmission axis is logarithmic. When the energy of the transmitting electrons is at the resonance peak ($E=0$), at $D=0$, transmission for this symmetric model assumes its maxi-

mum possible value of unity. With dephasing effects introduced (at higher values of D), transmission decreases. The coherent part of the transmission also decreases, even faster than the total transmission. At high values of D, transmission is dominated by its noncoherent contribution. Inspection of Fig. 2 helps to rationalize this drop in transmission. The DOS at the peak of the resonance at $D=0$ is quite high, resulting in strong transmission. As the dephasing parameter is increasing, electrons redistribute along the different energy channels. The DOS curve broadens, its value at $E=0$ eV diminishes, and therefore transmission decreases. As the DOS at resonance is at maximum value, the efficiency of phonon scattering [being proportional to $N(E)$] is high. The transmitted current becomes dominated by noncoherent channels even at moderate dephasing strengths. This behavior of the conductance shows signatures characteristic of metals. Far from the resonant peak (at $E/\Gamma=4$ in Fig. 3), transmission is much lower. With increasing values of D, transmission weakly rises, but remains dominated by the coherent channel. This behavior is reminiscent of insulators. The most interesting transmission curves appear at near-resonant energies (at $E/\Gamma=1.8$ in Fig. 3). At $D=0$ transmission is moderate; its value is in between those of the resonant and off-resonant cases. When the dephasing parameter is increased, both the total transmission and its coherent part at first increase, but, after reaching a maximum, decrease. This behavior is a mixture of the two cases discussed for the resonant and off-resonant cases, and a switch-over between the two conducting mechanisms is clearly exhibited. At low values of D, the rise of the transmission functions is moderate and they do not deviate much; current is dominated by the coherent channel. At a characteristic intermediate region of the dephasing parameter, the total transmission starts rising sharply, departing from the coherent contribution that reaches its maximum. Current becomes more and more noncoherent. Increasing D further, the transmission curves converge to the ones obtained for the resonant energy. This behavior can be associated with semiconductors.

We can see that the introduction of dephasing does not have a unique effect on the conductance of the system. If the charge carriers are in a resonant (high-DOS) region, transmission decreases. On the other hand, transmission can actually rise with dephasing at off-resonant (low-DOS) regions, as the outscattering of charge-carriers is outweighed by inscattering from higher DOS regions. The dominant mechanism of transmission is also affected by the resonant condition; current is more susceptible to become dominated by noncoherent channels at or near a resonance peak (or in a high-DOS region).

VI. EMERGENCE OF THE NONCOHERENT HOPPING MECHANISM

The significance of the noncoherent processes is determined by the dimensionless superoperator $\tilde{D}\tilde{U}$. Let us now consider [as suggested by the expansion in Eq. (55)] the action of $\tilde{D}\tilde{U}$ on an electron injected at one terminal, within the local dephasing model [Eq. (38)]. The matrix describing such an electron is essentially determined by the escape rate matrix, it is diagonal and local at the terminal site, and it does not involve coherences between different sites. The evolution operator $\tilde{U}$ delocalizes the electron, and coherences also develop; $\tilde{D}$, however, projects the electron state into its diagonal elements again. Subsequent action of $\tilde{D}\tilde{U}$ on the electron now localized at internal site(s) also projects onto diagonal electron states. $\tilde{D}\tilde{U}$ thus describes the propagation of the electron in the system, but it maps electronic populations to populations; coherences are suppressed. What we see is the emergence of the classical hopping mechanism, where only populations at different sites are taken into account with a probability distribution and quantum coherences need not be considered. In what follows, we will demonstrate how, in the limit of strong dephasing, our general results yield the noncoherent site-hopping behavior. We shall consider a homogeneous n-site chain with local dephasing and local terminal conducts. Strictly speaking, the limit we are taking in this section is justified when $t^2,\Gamma^2 \ll D$ (as will be apparent in our derivation). As we saw in the previous section, D can indeed be greater than Γ^2 for realistic junctions. For t^2 to be smaller than D, t should also be in the 0.1-eV regime or smaller. This value, although probably too low for a direct Huckel hopping parameter within a simple molecule, may actually be realistic when describing an effective hopping parameter between moities in an oligomeric molecular wire. In addition, we believe some of the conclusions of this section remain valid even if the $t^2 \ll D$ condition does not hold, but the chain is sufficiently long. This question will be addressed in a future publication with numerical investigation of arbitrarily long molecular wires.

First we have to solve the Dyson equation (44). Let us introduce the zeroth-order Green function G_0 as

$$G_0^r = (E - \tilde{D}G_0^r)^{-1}. \tag{71}$$

The superoperator $\tilde{D}$ projects onto a diagonal matrix in site representation; therefore, G_0^r is also diagonal, and in fact it is simply a multiple of the identity matrix $G_0^r = g_0 I$, where the complex number g_0 is determined by the equation

$$g_0 = 1/(E - Dg_0). \tag{72}$$

In the limit of strong dephasing, the other terms (H and Σ_{lead}) in Eq. (44) can be treated as perturbations. Writing $G^r = G_0^r + G_1^r = g_0 I + G_1^r$ where G_1^r is the perturbation in the Green function, we obtain the equation

$$g_0 I + G_1^r = g_0[I - g_0(\tilde{D}G_1^r + H + \Sigma_{lead})]^{-1}. \tag{73}$$

Expanding the inverse, keeping terms up to the first order in G_1^r and Σ, we arrive at the matrix equation for G_1^r:

$$G_1^r = g_0^2(\tilde{D}G_1^r + \Sigma_{lead}) + g_0^2 H + g_0^3 H^2 + \cdots . \tag{74}$$

The matrices $\tilde{D}G_1^r$ and Σ_{lead} are diagonal, and H is tridiagonal (with zero diagonal elements, as we take the site energies to be zero). The $1-n$ element of the Green function in lowest order thus comes from the term H^{n-1}: $[G^r]_{1n} = g_0^n t^{n-1}$. Using Eq. (56) and noting that Eq. (72) implies $|g_0|^2 = 1/D$, inde-

pendent of E, we obtain the coherent transmission in the strong dephasing limit:

$$T_{coh} = \frac{\Gamma_1\Gamma_2}{D}\left(\frac{t^2}{D}\right)^{n-1}. \tag{75}$$

This drops exponentially with chain length, and the decay length is inversely proportional to the dephasing parameter (to temperature when dephasing is induced by thermal phonons). It should be emphasized that the exponential length dependence obtained here for the *coherent* transmission is not related to the well-known exponential length dependence for the *total* transmission in the off-resonant, elastic case. The latter is a direct consequence of the tunneling mechanism. In the strong dephasing limit, the explanation is different: The coherent part of the transmission is due to electrons that never scatter in the chain. At each site, however, there is a probability of a scattering event. The flux of electrons that manage to avoid all such scattering events must therefore drop exponentially along the chain. Coherent transmission is not directly observable in conductance experiments, where the total current is measured. However, interactions mediated by the superexchange mechanism (such as Heisenberg coupling of electron spins at displaced radicals of a molecular chain) depend directly on the virtual transmission of *coherent* electrons. Such experiments have been performed,[68] and results agree with the exponential length dependence in Eq. (75).

To determine the total transmission, we need to calculate the Q matrix, introduced in Eq. (58). Starting from Eq. (74), we can express elements of the Green function and, from that, those of Q. In zeroth order, Q is determined by (the trivial) G_0^r, and itself is a multiple of the identity $Q=|g_0|^2 I = (1/D)I$. Up to second order in t, Q is tridiagonal. We obtain its diagonal and subdiagonal elements after substituting g_0 from Eq. (72):

$$[Q]_{jj} = \frac{1}{D} - \frac{t^2\eta_j}{D^2} - \frac{\Gamma_j}{D\sqrt{4D-E^2}}, \tag{76}$$

$$[Q]_{j+1,j} = [Q]_{j,j+1} = \frac{t^2}{D^2}. \tag{77}$$

The parameters here are $\eta_j=1$ for $j=1$ and n and $\eta_j=2$ for all other j. $\Gamma_j=\Gamma_1$ for $j=1$, $\Gamma_j=\Gamma_2$ for $j=n$, and $\Gamma_j=0$ for all other j, Γ_1 and Γ_2 are again the escape rates to the leads. Total transmission is essentially the power expansion of the matrix DQ [see Eq. (62)] Let us introduce the dimensionless parameters $p=t^2/D$, $q_1=\Gamma_1/(\sqrt{4D-E^2})$, and $q_2 = \Gamma_2/(\sqrt{4D-E^2})$ and write down the matrix DQ for, say, $n=4$:

$$DQ = \begin{pmatrix} 1-p-q_1 & p & 0 & 0 \\ p & 1-2p & p & 0 \\ 0 & p & 1-2p & p \\ 0 & 0 & p & 1-p-q_2 \end{pmatrix}. \tag{78}$$

We can see that this matrix describes the transfer of populations (probabilities) between sites in the chain. p is the hopping probability between neighboring sites, and q_1 and q_2 are hopping probabilities from the two terminal sites to the corresponding leads. Inversion of the matrix $1-DQ$ is tractable, and using Eq. (62) we obtain the total transmission in the strong dephasing limit:

$$T = \frac{\Gamma_1\Gamma_2}{D}\frac{p}{(n-1)q_1q_2 + p(q_1+q_2)}. \tag{79}$$

T is proportional to the conductance of the system. Substituting the expressions for p, q_1, and q_2, we express the reciprocal of the transmission which is proportional to resistance:

$$T^{-1} = \frac{1}{\sqrt{1-E^2/4D}}\frac{\sqrt{D}}{2}\left(\frac{1}{\Gamma_1}+\frac{1}{\Gamma_2}\right) + \frac{1}{1-E^2/4D}\frac{(n-1)D}{4t^2}. \tag{80}$$

We can see that the resistance is the sum of two terms. The first term is the contact resistance,[69] which depends on the molecule-contact couplings Γ_1 and Γ_2. Not surprisingly, this term is the reciprocal of the transmission we got for the single-site model in the strong dephasing limit [see Eqs. (70) and (66)]. Further assuming the molecular band is approximately half-filled (i.e., the Fermi energy lies close to the middle of the molecular band where $E=0$), the dimensionless prefactor goes to unity and we find that the contact resistance is proportional to the square root of D (to the square root of temperature in the case of dephasing assisted by thermal phonons). The second term in Eq. (80) does not depend on the molecule-contact couplings but rather on the intersite coupling t. Again, assuming $E=0$, we see that it is proportional to the chain length n and to the dephasing strength D (to the temperature). Of course, this is exactly what is expected for the Ohmic resistance of a classical wire.

VII. CONCLUSIONS

We have applied the nonequilibrium Green function formalism to study dephasing effects in molecular conduction. We investigated homogeneous, single-banded linear chains with tight-binding (Huckel) Hamiltonian. Starting from the self-consistent Born approximation, we derived phenomenological relationships determining the self-energies due to electron-phonon interactions in the limit of high phonon occupation numbers. The phenomenological self-energies are given as linear functionals of only their respective Green functions. Within this limit, the Dyson and Keldysh equations decouple, although both need to be solved in a self-consistent manner. As the self-energy is proportional to the electronic Green function, the dephasing efficiency due to phonons scales linearly with the local density of states. Scattering effects become more important at energy regions with higher DOS values. We derived the transmission function and its coherent part in the presence of dephasing effects. Our results are generalizations of the formula $T = \mathrm{Tr}[\Gamma_1 G^r \Gamma_2 G^a]$. We also generalized the formula $T = \Gamma_1\Gamma_2|[G^r]_{1n}|^2$ for locally coupled contacts.

We studied a one-site model with a single electronic level in detail. When dephasing effects are neglected, we recover

the usual Lorentzian line shape for the DOS whose width is determined by the coupling strength to the leads. In the other limit, when dephasing effects are very strong, we obtain a semicircular DOS curve, in accordance with DOS distributions for randomly disordered tight-binding chains. In this case the width is determined by the dephasing parameter. The transmission function obtained for the one-level model follows the general relationship derived for systems with proportionate couplings; it is proportional to the DOS. The noncoherent (inelastic) contribution to the transmission is weak in low-DOS regions, but dominates in high-DOS regions. Transmission (conductance) is affected by dephasing in a nontrivial manner. Stronger dephasing efficiency inhibits transmission (especially coherent transmission) at resonant energies, but it enhances both the total transmission and its coherent part in the off-resonant case. At near resonance, the transmission function is nonmonotonous, showing a maximum at a characteristic value of the dephasing parameter.

Finally, we investigated long molecular chains in the limit of strong local dephasing. In this case, quantum coherences between different sites were found to be destroyed. The description collapses into what can be identified as the transfer matrix describing hopping probabilities between electronic populations at neighboring sites and those between terminal sites and the corresponding contacts. We find that the coherent part of the transmission in this limit decays exponentially along the chain. The reciprocal of the total transmission, which is proportional to the resistance of the wire, is the sum of two terms: The contact resistance does not depend on the length of the chain, only on the molecule-contact coupling. We find that it is proportional to the square root of the temperature. The other term that depends on molecular parameters shows signatures of the Ohmic resistance of an ordinary wire; it is proportional to the chain length and to the temperature.

We have demonstrated that the nonequilibrium Green function technique can be used as a powerful first-principles analytic tool to study nonelastic effects in molecular conduction. In the limits of Coulomb blockade and other strong correlation phenomena, local dephasings may provide a totally different mechanistic modification. Analysis of this situation will be reported subsequently.

ACKNOWLEDGMENTS

We are grateful to M. Galperin, A. Xue, and A. Nitzan for helpful remarks; this work was supported by the DARPA MoleApps program, by the NASA URETI program, and by the DOD MURI/DURINT program.

[1] C. Joachim, J. K. Gimzewski, and A. Aviram, Nature (London) **408**, 541 (2000).
[2] A. Nitzan, Annu. Rev. Phys. Chem. **52**, 681 (2001).
[3] A. Nitzan and M. A. Ratner, Science **300**, 1384 (2003).
[4] *Introduction to Nanoscale Science and Technology*, edited by M. Di Ventra, S. Evoy, and J. R. Heflin (Kluwer Academic, Norwell, 2004).
[5] *Molecular Nanoelectronics*, edited by M. A. Reed and T. Lee (American Scientific, Stevenson Ranch, 2003).
[6] See *Molecular Electronics: Science and Technology*, edited by A. Aviram and M. A. Ratner [Ann. N.Y. Acad. Sci. **852** (1998)]; *Molecular Electronics II*, edited by A. Aviram, M. A. Ratner, and V. Mujica [*ibid.* **960** (2002)]; *Molecular Electronics III*, edited by J. Reimers, C. Picconatto, J. Ellenbogen, and R. Shashidhar [*ibid.* **1006** (2003)].
[7] S. Datta, *Quantum Transport, Atom to Transistor* (Cambridge University Press, Cambridge, England, 2005).
[8] D. J. Wold, R. Haag, M. A. Rampi, and C. D. Frisbie, J. Phys. Chem. B **106**, 2813 (2002).
[9] J. G. Kushmerick, D. B. Holt, J. C. Yang, J. Naciri, M. H. Moore, and R. Shashidhar, Phys. Rev. Lett. **89**, 086802 (2002).
[10] J. Chen, J. Su, W. Wang, and M. A. Reed, Physica E (Amsterdam) **16**, 17 (2003).
[11] J. Reichert, H. B. Weber, M. Mayor, and H. von Lohneysen, Appl. Phys. Lett. **82**, 4137 (2003).
[12] S. Kubatkin, A. Danilov, M. Hjort, J. Cornil, J.-L. Bredas, N. Stuhr-Hansen, P. Hedegard, and T. Bjornholm, Nature (London) **425**, 698 (2003).
[13] V. Mujica, M. Kemp, and M. A. Ratner, J. Chem. Phys. **101**, 6849 (1994).
[14] V. Mujica, M. Kemp, and M. A. Ratner, J. Chem. Phys. **101**, 6856 (1994).
[15] E. G. Emberly and G. Kirczenow, Phys. Rev. B **64**, 125318 (2001).
[16] C. Gonzalez, V. Mujica, and M. A. Ratner, in *Molecular Electronics II* [Ann. N.Y. Acad. Sci. **960**, 163 (2002)].
[17] A. W. Ghosh, P. Damle, S. Datta, and A. Nitzan, MRS Bull. **29**, 391 (2004).
[18] J. Taylor, H. Guo, and J. Wang, Phys. Rev. B **63**, 245407 (2001).
[19] M. Di Ventra and N. D. Lang, Phys. Rev. B **65**, 45402 (2001).
[20] Y. Q. Xue, S. Datta, and M. A. Ratner, Chem. Phys. **281**, 151 (2002).
[21] M. Brandbyge, J.-L. Mozos, P. Ordejon, J. Taylor, and K. Stokbro, Phys. Rev. B **65**, 165401 (2002).
[22] S. T. Pantelides, M. Di Ventra, N. D. Lang, and S. N. Rashkeev, IEEE Trans. Nanotechnol. **1**, 86 (2002).
[23] S.-H. Ke, H. U. Baranger, and W. Yang, Phys. Rev. B **70**, 085410 (2004).
[24] W. B. Davis, W. A. Svec, and M. A. Ratner, and M. R. Wasielewski, Nature (London) **396**, 60 (1998).
[25] A. L. Burin, Y. A. Berlin, and M. A. Ratner, J. Phys. Chem. A **105**, 2652 (2001).
[26] H. Ness and A. J. Fisher, Chem. Phys. **281**, 279 (2002).
[27] J. Lehmann, G.-L. Ingold, and P. Hanggi, Chem. Phys. **281**, 199 (2002).
[28] D. Segal and A. Nitzan, J. Chem. Phys. **117**, 3915 (2002).
[29] H. M. Pastawski, L. E. F. F. Torres, and E. Medina, Chem. Phys. **281**, 257 (2002).
[30] V. Mujica, A. Nitzan, S. Datta, M. A. Ratner, and C. P. Kubiak, J. Phys. Chem. B **107**, 91 (2003).

[31] M. Abu-Hilu and U. Peskin, Chem. Phys. **296**, 231 (2004).
[32] E. G. Petrov, V. May, and P. Hanggi, Chem. Phys. **296**, 251 (2004).
[33] X. H. Qiu, G. V. Nazin, and W. Ho, Phys. Rev. Lett. **92**, 206102 (2004).
[34] B. C. Stipe, M. A. Rezaei, W. Ho, S. Gao, M. Persson, and B. I. Lundqvist, Phys. Rev. Lett. **78**, 4410 (1997).
[35] T. Seideman, J. Mod. Opt. **50**, 2393 (2003).
[36] T. Seideman and H. Guo, J. Theor. Comput. Chem. **2**, 439 (2003).
[37] J. G. Kushmerick, J. Lazorcik, C. H. Patterson, R. Shashidhar, D. S. Seferos, and G. C. Bazan, Nano Lett. **4**, 639 (2004).
[38] W. Y. Wang, T. Lee, I. Kretzschmar, and M. A. Reed, Nano Lett. **4**, 643 (2004).
[39] Y. Selzer, M. A. Cabassi, T. S. Mayer, and D. L. Allara, Nanotechnology **15**, S483 (2004).
[40] S. Alavi, B. Larade, J. Taylor, H. Guo, and T. Seideman, Chem. Phys. **281**, 293 (2002).
[41] A. Troisi, A. Nitzan, and M. A. Ratner, J. Chem. Phys. **119**, 5782 (2003).
[42] M. Di Ventra, Y. C. Chen, and T. N. Todorov, Phys. Rev. Lett. **92**, 176803 (2004).
[43] A. Troisi and M. A. Ratner (unpublished).
[44] M. Galperin, M. A. Ratner, and A. Nitzan, Nano Lett. **4**, 1605 (Communication) (2004).
[45] M. Galperin, M. A. Ratner, and A. Nitzan, J. Chem. Phys. **121**, 11965 (2004).
[46] L. V. Keldysh, Sov. Phys. JETP **20**, 1018 (1965).
[47] L. P. Kadanoff and G. Baym, *Quantum Statistical Mechanics: GReen's Function Methods in Equilibrium and Nonequilibrium Problems* (Benjamin, Reading, MA, 1962).
[48] M. Wagner, Phys. Rev. B **44**, 6104 (1991).
[49] S. Datta, *Electronic Transport in Mesoscopic Systems* (Cambridge University Press, Cambridge, England, 1995).
[50] T. Seideman and W. H. Miller, J. Chem. Phys. **97**, 2499 (1992).
[51] E. G. Emberly and G. Kirczenow, in *Molecular Electronics: Science and Technology* [Ann. N.Y. Acad. Sci. 852, 54 (1998)].
[52] H. Ness and A. J. Fisher, Phys. Rev. Lett. **83**, 452 (1999).
[53] N. S. Hush, in *Molecular Electronics III* [Ann. N.Y. Acad. Sci.1006, 1 (2003)].
[54] K. Stokbro, J. Taylor, M. Brandbyge, and P. Ordejon, in *Molecular Electronics III* [Ann. N.Y. Acad. Sci.1006, 212 (2003)].
[55] M. Buttiker, IBM J. Res. Dev. **32**, 63 (1988).
[56] H. J. Lee and W. Ho, Science **286**, 1719 (1999).
[57] R. Lake, G. Klimeck, R. C. Bowen, and D. Jovanovic, J. Appl. Phys. **81**, 7845 (1997).
[58] S. Datta and R. K. Lake, Phys. Rev. B **44**, R6538 (1991).
[59] S. Datta, Phys. Rev. B **46**, 9493 (1992).
[60] S. Datta, Phys. Rev. B **45**, 1347 (1992).
[61] H. Haug and A.-P. Jauho, *Quantum Kinetics in Transport and Optics of Semiconductors* (Springer-Verlag, Berlin, 1996).
[62] P. F. Barbara, T. J. Meyer, and M. A. Ratner, J. Phys. Chem. **100**, 13148 (1996).
[63] Y. A. Berlin, G. R. Hutchison, P. Rempala, M. A. Ratner, and J. Michl, J. Phys. Chem. A **107**, 3970 (2003).
[64] V. Lemaur, D. A. da Silva Filho, V. Coropceanu, M. Lehmann, Y. Geerts, J. Piris, M. G. Debije, A. M. van de Craats, K. Senthilkumar, L. D. A. Siebbeles, J. M. Warman, J. L. Bredas, and J. Cornil, J. Am. Chem. Soc. **126**, 3271 (2004).
[65] F. J. Wegner, Phys. Rev. B **19**, 783 (1979).
[66] M. L. Mehta, *Random Matrices* (Academic Press, New York, 1991).
[67] E. Gudowska-Nowak, G. Papp, and J. Brickmann, Chem. Phys. **232**, 247 (1998).
[68] E. A. Weiss, M. J. Ahrens, L. E. Sinks, A. V. Gusev, M. A. Ratner, and M. R. Wasielewski, J. Am. Chem. Soc. **126**, 5577 (2004).
[69] R. J. Chesterfield, J. C. McKeen, C. R. Newman, C. D. Frisbie, P. C. Ewbank, K. R. Mann, and L. L. Miller, J. Appl. Phys. **95**, 6396 (2004).